PHYSICAL REVIEW B VOLUME 18, NUMBER 12 15 DECEMBER 1978

Electron scattering interaction with coupled plasmon–polar-phonon modes in degenerate semiconductors

M. E. Kim*, A. Das, and S. D. Senturia
Department of Electrical Engineering and Computer Science and Center for Materials Science and Engineering, Massachusetts Institute of Technology, Cambridge, Massachusetts 02139
(Received 6 June 1978)

The scattering interaction of Bloch electrons with the coupled systems of electrons and longitudinal-optical phonons in degenerate polar semiconductors is investigated. At degenerate carrier concentrations (10^{17}–10^{18} cm^{-3} in IV–VI and III–V compounds) the free-carrier plasma frequency is comparable to the LO-phonon frequency. This gives rise to electron scattering by strongly coupled plasmon–LO-phonon modes whose resonance frequencies are highly broadened in the particle-hole excitation (Landau damping) region. A generalized expression for the scattering lifetime taking these effects into account is derived in terms of a dielectric response formalism within the random-phase approximation. The factor $\mathrm{Im}(1/\epsilon_T)$ appearing in this treatment, where ϵ_T is the coupled-system dielectric function, modifies the bare Coulomb potential, and together they determine the effective scattering strength of the coupled modes. In the Landau-damping region the scattering strength is highly dispersive with respect to energy and momentum transfers. Calculations that illustrate these interaction effects are performed for PbTe and GaAs.

I. INTRODUCTION

In ionic (polar) semiconductors such as the IV-VI and the III-V compounds, the combined role of the longitudinal-optical (polar) phonon and the charge-carrier systems has long been recognized as important in characterizing electronic relaxation, transport, and optical phenomena. The LO phonons are coupled through long-range polarization fields to the free-carrier system which includes the collective plasma modes and the particle-hole excitations. This coupling gives rise to hybrid plasmon–LO-phonon modes and to the damping of these modes by the particle-hole excitations (Landau damping). Landau damping, particularly important in transport processes, broadens out the coupled-mode resonance frequencies with which Bloch electrons can interact and provides an indirect mechanism for single-particle, electron-electron interactions to contribute to transport properties.

Until now, treatment of these interrelated interaction effects in describing the Bloch electron lifetime has been limited to various approximations. The unscreened electron–LO-phonon (Fröhlich) interaction has been thoroughly investigated.[1-3] Ehrenreich formulated the electron scattering lifetime associated with a screened LO phonon in a nondegenerate semiconductor using a self-consistent-field approach. However, the effects of particle-hole damping were neglected.[4] Charge carrier scattering by polar phonons in degenerate semiconductors has only been treated in the undamped, highly screened case within the quasistatic approximation.[3,5] Single-particle, electron-electron scattering in semiconductors has been limited to statically screened interactions.[6,7]

In this paper the problem is treated in a generalized manner within the framework of the random-phase approximation (RPA).[8] We consider degenerate carrier concentrations such that the free-carrier plasma frequency is comparable to the LO-phonon frequency—a situation which gives rise to strongly coupled plasmon–LO-phonon modes. The corresponding carrier concentrations for the IV-VI and III-V semiconductors are in the range $\sim 10^{17}$–10^{18} cm^{-3}, and still form a high-density gas because of the small effective masses (m^*) and the large dielectric constants (ϵ_∞).[9] [The effective interelectron radius

$$r_s^* = (3/4\pi n)^{1/3}(m^* e^2/\hbar^2 \epsilon_\infty) \lesssim 0.1$$

corresponding to carrier concentrations $n \gtrsim 10^{17}$ cm^{-3}.] The tractable RPA seems to be appropriate.[10,11]

In Sec. II the Bloch electron scattering lifetime arising from the electron-electron and electron–LO-phonon interactions is derived using diagrammatic techniques. It is well known that for electrostatic scattering processes, lifetimes become functions of the imaginary part of a reciprocal longitudinal dielectric function.[12,13] In the RPA the susceptibility of the coupled system is just the sum of the susceptibilities of the system components.[14] Thus, in our case the reciprocal of the lifetime is proportional to $\mathrm{Im}(1/\epsilon_T)$, where $\epsilon_T = \epsilon_e + \epsilon_L - 1$, and ϵ_e and ϵ_L are the respective electronic and lattice dielectric functions. The generalized scattering lifetime is shown to reduce to familiar expressions in appropriate limiting cases.

In Sec. III we study the dispersion and damping of the coupled plasmon–LO-phonon modes in PbTe and GaAs using the Lindhard dielectric function[10] to describe the free-carrier response. The electron–coupled-mode scattering strength, defined by the bare Coulomb potential as modified by $\mathrm{Im}(1/\epsilon_T)$, is studied numerically as a function of both energy and momentum transfers. In the Landau-damping regime the scattering strength is highly dispersive. The scattering of electrons by the broadened couple modes in this region provides a mechanism for electron-electron nonumklapp processes to contribute to transport properties. For low-field transport the mode broadening could make the low-energy tail of the scattering strength contribute appreciably to scattering via the boson population factor. In high-field transport it seems essential to treat the role of broadened coupled modes in characterizing hot electrons and saturation velocities.

Useful application of the scattering formalism presented here will be illustrated in a separate work characterizing low-field transport effects in narrow-gap semiconductors $Pb_{1-x}Sn_xTe$.

II. GENERALIZED SCATTERING LIFETIME

In the standard second-quantization notation the Hamiltonian for the system of electrons and LO phonons interacting through electrostatic forces is as follows:

$$\mathcal{H}=\sum_{\vec{k},n} E_{\vec{k},n}c^\dagger_{\vec{k},n}c_{\vec{k},n}+\frac{1}{2}\sum_{\vec{q}}(P^\dagger_{\vec{q}}P_{\vec{q}}+\omega^2_{\mathrm{TO}}Q^\dagger_{\vec{q}}Q_{\vec{q}})+\frac{1}{2}\sum_{\vec{q}}(\Omega^0_L)^2Q^\dagger_{\vec{q}}Q_{\vec{q}}+\sum_{\vec{q}}\left(\frac{2\pi e^2}{q^2}\right)\rho_{e,\vec{q}}\,\rho^\dagger_{e,\vec{q}}-i\Omega^0_L\sum_{\vec{q}}\left(\frac{4\pi e^2}{q^2}\right)^{1/2}\left(\frac{\vec{q}\cdot\hat{e}_{\vec{q}}}{q}\right)\rho_{e,\vec{q}}Q^\dagger_{\vec{q}}\,. \tag{1}$$

The first term is the Hamiltonian for the Bloch electrons; the second term is the LO-phonon Hamiltonian in the absence of long range electrostatic interactions; the third term is the Hamiltonian for LO-LO electrostatic interactions; the fourth and fifth terms are, respectively, Hamiltonians for electron-electron and electron–LO-phonon electrostatic interactions. The Hamiltonian can be readily derived from elementary electrostatic considerations; the form of the electron–LO-phonon interaction is somewhat different from that one usually encounters in the literature.[15,16] Here, $c_{\vec{k},n}$ ($c^\dagger_{\vec{k},n}$) is the annihilation (creation) operator for the Bloch state $|\vec{k},n\rangle$ with energy $E_{\vec{k},n}$; $Q_{\vec{q}}$ and $P_{\vec{q}}$ are the coordinate and momentum operators for the LO phonons;

$$\Omega^0_L=(4\pi Ne^{*2}/M)^{1/2}=[\epsilon_\infty(\omega^2_{\mathrm{LO}}-\omega^2_{\mathrm{TO}})]^{1/2}$$

is the unscreened ionic plasma frequency; N is the number of unit cells; e^* is the effective ionic charge; and M is the reduced ionic mass. Also,

$$\rho_{e,\vec{q}}=\sum_{\vec{k},n,n'}F^{nn'}_{\vec{k},\vec{k}-\vec{q}}c^\dagger_{\vec{k}-\vec{q},n'}c_{\vec{k},n}$$

is the Fourier component of the electron density fluctuations. $F^{nn'}_{\vec{k},\vec{k}-\vec{q}}$ is the matrix element $\langle\vec{k}-\vec{q},n'|e^{-i\vec{q}\cdot\vec{r}}|\vec{k},n\rangle$. $\hat{e}_{\vec{q}}$ is the unit longitudinal polarization vector for the LO phonons.

From Eq. (1) we observe that the total Hamiltonian for electrostatic scattering of electrons in band n is

$$\mathcal{H}'_s=\sum_{\vec{k},\vec{q}}[\Gamma_\rho(\vec{q})\rho_{e,-\vec{q}}+\Gamma_Q(\vec{q})Q_{-\vec{q}}]F^{nn}_{\vec{k},\vec{k}-\vec{q}}c^\dagger_{\vec{k}-\vec{q},n}c_{\vec{k},n}\,. \tag{2}$$

Here

$$\Gamma_\rho(\vec{q})=4\pi e^2/q^2 \tag{3a}$$

and

$$\Gamma_Q(\vec{q})=-i\Omega^0_L\left(\frac{4\pi e^2}{q^2}\right)^{1/2}\left(\frac{\vec{q}\cdot\hat{e}_{\vec{q}}}{q}\right). \tag{3b}$$

From the golden rule the reciprocal of the lifetime for the Bloch state $|\vec{k},n\rangle$ due to electrostatic scattering for all wave-vector transfers within the Brillouin zone is

$$\tau^{-1}(\vec{k},n)=\frac{2\pi}{\hbar}\int_{-\vec{q}_c}^{\vec{q}_c}\frac{d\vec{q}}{(2\pi)^3}|\langle\vec{k}-\vec{q},n|\mathcal{H}'_s|\vec{k},n\rangle|^2\times\delta(\hbar\omega+E_{\vec{k}-\vec{q},n}-E_{\vec{k},n})\,, \tag{4}$$

where $\vec{q}_c$ is the cutoff wave vector for the zone.

We can now use the standard Van Hove technique[17] to recast expression (4) into the following form:

$$\tau^{-1}(\vec{k},n)=\frac{2\pi}{\hbar}\int_{-\vec{q}_c}^{\vec{q}_c}\frac{d\vec{q}}{(2\pi)^3}\int_{-\infty}^{\infty}\frac{d\hbar\omega}{2\pi}f_{\vec{k},n}(1-f_{\vec{k}-\vec{q},n})(1+n_\omega)|F^{nn}_{\vec{k},\vec{k}-\vec{q}}|^2\times\left(\sum_{i,j=\rho,Q}\Gamma_i(\vec{q})\Gamma^*_j(\vec{q})P_{ij}(\vec{q},\omega)\right)\delta(\hbar\omega+E_{\vec{k}-\vec{q},n}-E_{\vec{k},n})\,, \tag{5}$$

where $f_{\vec{k},n}$ and n_ω are the respective fermion and boson distribution functions; $P_{ij}(\vec{q},\omega)$ is the spectral density function defined through the fluctuation-dissipation theorem

$$P_{ij}(\vec{q},\omega)=2\,\mathrm{Im}[\mathfrak{D}_{ij}(\vec{q},\omega)]\,. \tag{6}$$

Here, $\mathfrak{D}_{ij}(\vec{q},\omega)$ is the Fourier transform of the retarded Green's function; e.g.,

$$\mathfrak{D}_{\rho Q}(\vec{q},t)=-i\Theta(t)\langle|[\rho_{\vec{q}}(t),Q_{\vec{q}}^{\dagger}(0)]|\rangle\,,$$

where $\Theta(t)$ denotes the unit-step function. Expression (5) could have been obtained by calculating the self-energy of the Bloch electron in the presence of the interactions represented by $\mathcal{H}_s'$, in which case we would have

$$\tau^{-1}(\vec{k},n)=\sum_{i,j=\rho,Q}\mathrm{Im}(\Sigma_{ij})\,, \tag{7}$$

where the self-energy functions Σ_{ij} are shown in the top line of Fig. 1.

Now we calculate the Green's functions $\mathfrak{D}_{ij}(\vec{q},\omega)$ in the random-phase approximation. The RPA diagram expansions are shown in Fig. 1. $\mathfrak{D}^0_{ij}(\vec{q},\omega)$ are the zeroth-order Green's functions. From the diagram expansions, using standard rules,[18] we obtain the following expressions:

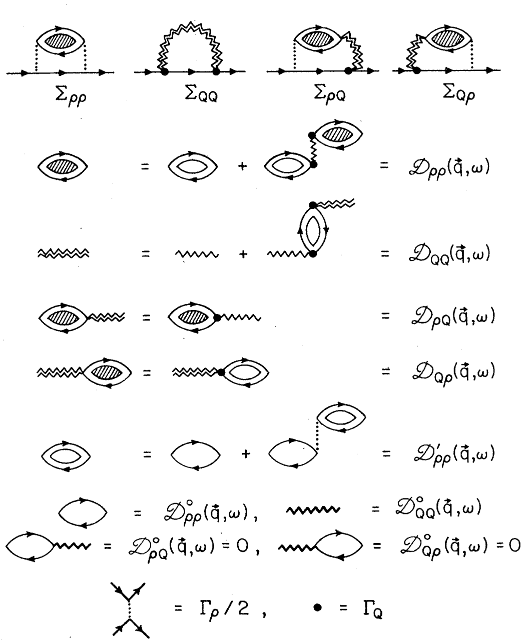

FIG. 1. Diagram expansions in the random-phase approximation. Σ_{ij} are the self-energy interactions. $\mathfrak{D}_{ij}(\vec{q},\omega)$ are the Fourier transforms of the retarded Green's functions. $\mathfrak{D}'_{\rho\rho}(\vec{q},\omega)$ is the RPA polarization Green's function and $\mathfrak{D}^0_{ij}(\vec{q},\omega)$ are the zeroth-order Green's functions. Γ_ρ is the electron-electron interaction and Γ_Q is the electron-phonon interaction.

$$\mathfrak{D}_{\rho\rho}(\vec{q},\omega)=\hbar\left(\frac{q^2}{4\pi e^2}\right)\frac{[1-\epsilon_e(\vec{q},\omega)]\epsilon_L(\vec{q},\omega)}{\epsilon_T(\vec{q},\omega)}\,,$$

$$\mathfrak{D}_{QQ}(\vec{q},\omega)=\hbar\left(\frac{1}{\Omega_L^{02}}\right)\frac{[1-\epsilon_L(\vec{q},\omega)]\epsilon_e(\vec{q},\omega)}{\epsilon_T(\vec{q},\omega)}\,,$$

$$\mathfrak{D}_{\rho Q}(\vec{q},\omega)=-i\hbar\left(\frac{1}{\Omega_L^0}\right)\left(\frac{q^2}{4\pi e^2}\right)^{1/2}\left(\frac{\vec{q}\cdot\hat{e}_{\vec{q}}}{q}\right)\times\frac{[1-\epsilon_e(\vec{q},\omega)][1-\epsilon_L(\vec{q},\omega)]}{\epsilon_T(\vec{q},\omega)}\,, \tag{8}$$

$$\mathfrak{D}_{Q\rho}(\vec{q},\omega)=-\mathfrak{D}_{\rho Q}(\vec{q},\omega)\,,$$

where

$$\epsilon_e(\vec{q},\omega)=1-\frac{4\pi e^2}{q^2}\sum_{\vec{k};n,n'}|F^{nn'}_{\vec{k},\vec{k}-\vec{q}}|^2\times\frac{f_{\vec{k}-\vec{q},n'}-f_{\vec{k},n}}{\hbar\omega+E_{\vec{k}-\vec{q},n'}-E_{\vec{k},n}+i0^{+}} \tag{9}$$

is the RPA electronic dielectric function,

$$\epsilon_L(\vec{q},\omega)=1-\frac{\Omega_L^{02}}{\omega^2-\omega_{\mathrm{TO}}^2}=1-\epsilon_\infty\left(\frac{\omega_{\mathrm{LO}}^2-\omega_{\mathrm{TO}}^2}{\omega^2-\omega_{\mathrm{TO}}^2}\right) \tag{10}$$

is the dielectric function of the lattice alone, and finally

$$\epsilon_T(\vec{q},\omega)=\epsilon_e(\vec{q},\omega)+\epsilon_L(\vec{q},\omega)-1 \tag{11}$$

is the total dielectric function of the coupled system. The fact that the susceptibilities add in the RPA was noted by Varga.[14] Damping of the coupled system in our treatment is due only to decay into particle-hole excitations (Landau damping).[19] It occurs in the wave-vector region where scattering, affecting transport, can be important. Collisional damping processes, which can also affect the coupled mode behavior,[15,20] will not be treated in this work.

Substituting Eqs. (6) and (8) in (5), we obtain

$$\tau^{-1}(\vec{k},n)=\frac{2\pi}{\hbar}\int\frac{d\vec{q}}{(2\pi)^3}\int\frac{d\hbar\omega}{2\pi}f_{\vec{k},n}(1-f_{\vec{k}-\vec{q},n})\times(1+n_\omega)|F^{nn}_{\vec{k},\vec{k}-\vec{q}}|^2\times\frac{4\pi e^2}{q^2}\left\{-\mathrm{Im}\left[\frac{1}{\epsilon_T(\vec{q},\omega)}\right]\right\}\times\delta(\hbar\omega+E_{\vec{k}-\vec{q},n}-E_{\vec{k},n})\,. \tag{12}$$

Expression (12) describes the generalized scattering lifetime and reduces to familiar results, the unscreened Fröhlich scattering and the highly screened LO-phonon scattering for the respective limits of very low and very high carrier concentrations.

If the free-carrier density is vanishingly small [$\omega_p^0\ll\omega_{\mathrm{LO}}$, where $\omega_p^0=(4\pi ne^2/m^*\epsilon_\infty)^{1/2}$ is the screened free-carrier plasma frequency], then $\epsilon_e(\vec{q},\omega)\simeq\epsilon_\infty$ and

$$-\mathrm{Im}[1/\epsilon_T(\vec{q},\omega)] = \frac{\pi}{2}\,\omega\left(\frac{1}{\epsilon_\infty}-\frac{1}{\epsilon_0}\right)\times[\delta(\omega-\omega_{\mathrm{LO}})-\delta(\omega+\omega_{\mathrm{LO}})]\,. \quad (13)$$

Equation (12) then yields the well-known expression[3]

$$\tau^{-1}(\vec{k},n)=\frac{2\pi}{\hbar}\int\frac{d\vec{q}}{(2\pi)^3}f_{\vec{k},n}\,(1-f_{\vec{k}-\vec{q},n})(1+n_{\omega_{\mathrm{LO}}})\times|F^{nn}_{\vec{k},\vec{k}-\vec{q}}|^2\,\frac{4\pi e^2}{q^2}\left[\frac{\hbar\omega_{\mathrm{LO}}}{2}\left(\frac{1}{\epsilon_\infty}-\frac{1}{\epsilon_0}\right)\right]\times\delta(\hbar\omega_{\mathrm{LO}}+E_{\vec{k}-\vec{q},n}-E_{\vec{k},n})\,. \quad (14)$$

For high carrier densities ($\omega_p^0 \gg \omega_{\mathrm{LO}}$) the free-carrier contribution to $\epsilon_e(\vec{q},\omega)$ can be treated in the quasistatic limit ($\omega\to 0$),

$$\epsilon_e(\vec{q},\omega)=\epsilon_\infty+(1+q_s^2/q^2)-1\,, \quad (15)$$

where q_s is the Fermi-Thomas wave vector. In this limit the LO phonons are highly dispersive in the small-q region with the dispersion relation given by[21]

$$\omega_q=\left(\frac{q^2\omega_{\mathrm{LO}}^2+q_s^2\omega_{\mathrm{TO}}^2}{q^2+q_s^2}\right)^{1/2}. \quad (16)$$

Expression (15) yields

$$-\mathrm{Im}[1/\epsilon_T(\vec{q},\omega)]=\frac{\omega_{\mathrm{LO}}^2q^4}{(q^2+q_s^2)^2}\left(\frac{1}{\epsilon_\infty}-\frac{1}{\epsilon_0}\right)\times\frac{\pi}{2\omega_q}[\delta(\omega-\omega_q)-\delta(\omega+\omega_q)] \quad (17)$$

and the well-known expression[3]

$$\tau^{-1}(\vec{k},n)=\frac{2\pi}{\hbar}\int\frac{d\vec{q}}{(2\pi)^3}f_{\vec{k},n}(1-f_{\vec{k}-\vec{q},n})(1+n_{\omega_q})\,|F^{nn}_{\vec{k},\vec{k}-\vec{q}}|^2\,\frac{4\pi e^2}{q^2}\left[\frac{q^4}{(q^2+q_s^2)^2}\,\frac{\hbar\omega_{\mathrm{LO}}^2}{2\omega_q}\left(\frac{1}{\epsilon_\infty}-\frac{1}{\epsilon_0}\right)\right]\delta(\hbar\omega_q+E_{\vec{k}-\vec{q},n}-E_{\vec{k},n})\,. \quad (18)$$

III. PROPERTIES OF THE GENERALIZED SCATTERING LIFETIME

In this section we examine the reciprocal scattering lifetime, Eq. (12), with respect to specific models which facilitate quantitative calculations and give insight to the more general qualitative properties. These include the use of the wave-vector-independent lattice dielectric function, Eq. (10), and the Lindhard dielectric function to approximate the intraband component of the RPA function, Eq. (9). In the wave-vector region of interest for degenerate carrier distributions, it is essential to take the dispersion and Landau damping into account. The simplest model which does so is the Lindhard function, derived for a free-electron gas at $T=0$, which is also assumed to approximate the finite temperature, degenerate statistics case.

The total electronic dielectric function in terms of the real and imaginary parts of the Lindhard function,[10] denoted by $\epsilon_r^{eL}(\vec{q},\omega)$ and $\epsilon_i^{eL}(\vec{q},\omega)$, can be written

$$\epsilon_e(\vec{q},\omega)=[\epsilon_\infty+\epsilon_r^{eL}(\vec{q},\omega)-1]+i[\epsilon_i^{eL}(\vec{q},\omega)]\,, \quad (19)$$

where

$$\epsilon_r^{eL}(\vec{q},\omega)=1+D\left(\frac{4\pi e^2}{q^2}\,\frac{m^*k_F}{\hbar^2 2\pi^2}\right)\left\{1+\frac{1}{2q'}\left[1-\left(\frac{\nu'}{q'}+\frac{q'}{2}\right)^2\ln\left|\frac{1+(\nu'/q'+\frac{1}{2}q')}{1-(\nu'/q'+\frac{1}{2}q')}\right|\right]-\frac{1}{2q'}\left[1-\left(\frac{\nu'}{q'}-\frac{q'}{2}\right)^2\ln\left|\frac{1+(\nu'/q'-\frac{1}{2}q')}{1-(\nu'/q'-\frac{1}{2}q')}\right|\right]\right\}, \quad (20)$$

$q'=q/k_F$, $\nu'=m^*\hbar\omega/\hbar^2k_F^2$

and

$$\epsilon_i^{eL}(\vec{q},\omega)=\begin{cases} D\left(\frac{4\pi e^2}{q^2}\right)\frac{m^*k_F}{\hbar^2 2\pi}\frac{\nu'}{q'}, & q<2k_F,\ 0<\hbar\omega<-\frac{\hbar^2}{2m^*}(q^2-2qk_F)\\ D\left(\frac{4\pi e^2}{q^2}\right)\frac{m^*k_F^2}{\hbar^2 4\pi q}\left[1-\left(\frac{\nu'}{q'}-\frac{q'}{2}\right)^2\right], & 0<-\frac{\hbar^2}{2m^*}(q^2-2qk_F)<\hbar\omega<\frac{\hbar^2}{2m^*}(q^2+2qk_F)\\ 0, & \hbar\omega>\frac{\hbar^2}{2m^*}(q^2+2qk_F)\\ 0, & q>2k_F,\ \hbar\omega<\frac{\hbar^2}{2m^*}(q^2-2qk_F)\,. \end{cases} \quad (21)$$

ϵ_r^{eL} and ϵ_i^{eL} have been modified for a semiconductor, where D is the number of equivalent charge carrier pockets in the Brillouin zone; m^* and k_F are, respectively, the effective mass and the Fermi wave vector appropriately averaged over the carrier pocket. ϵ_i^{eL} corresponds to damping of the collective electron modes by intraband particle-hole excitations. (Collisional damping will be neglected in this treatment.) The different damping forms and boundaries in Eq. (21) arise from energy and momentum selection rules at $T=0$. The existence of zero-damping regions is a consequence of the RPA pair approximation, given by $\mathfrak{D}'_{\rho\rho}(\vec{q}, \omega)$ in Fig. 1. Higher-order diagrams would allow the plasmons to decay for all q, however, at high effective carrier densities these processes are relatively weak.[22] Also finite temperatures would smear out these boundaries to some degree.

To investigate the behavior of the generalized scattering lifetime, we focus primarily on the semiconductor PbTe. GaAs is also considered for comparison. The typically encountered degenerate carrier concentration 10^{17}–10^{18} cm^{-3} in PbTe yield plasma frequencies $0.75 \lesssim \omega_p^0/\omega_{LO} \lesssim 2.2$. Furthermore, the large difference between ω_{LO} and ω_{TO} is indicative of relatively strong electrostatic interactions between the LO phonons. Also the small carrier effective masses give rise to particle-hole excitation effects at low-energy and wave-vector transfers. These properties are expected to lead to strong coupling of the LO phonons with the free-carrier system and large dispersion of the coupled modes and of the scattering strength associated with these modes.

In PbTe the charge carrier pockets (nonparabolic in behavior) are described by four ellipsoids of revolution at the L point of the fcc crystal Brillouin zone.[23] For carrier concentrations $\lesssim 5\times10^{17}$ cm^{-3}, the longitudinal Fermi wave vector (in the L direction) is a few percent of the Brillouin-zone width, and the dispersion of the optical-phonon modes can be neglected. For PbTe, the average susceptibility mass (based on a nonparabolic $\vec{k}\cdot\vec{p}$ model) and an average Fermi wave vector (based on spherical carrier pockets) are used for m^* and k_F, respectively. The optical-phonon energies are taken as $\hbar\omega_{LO}=13.5$ meV and $\hbar\omega_{TO}=2.5$ meV, representative of inelastic-neutron-scattering data[24] and fits to optical data,[25,26] while the value of ϵ_∞ taken is 39 (5 °K).[27] GaAs has a single carrier pocket at the Γ point and thus the average Fermi wave vector is ~1.5 times larger than that of PbTe for the same carrier concentration. The effective masses of GaAs and PbTe are comparable. However, the optical-phonon energies and ϵ_∞ are quite different: $\hbar\omega_{LO}=36.3$ meV, $\hbar\omega_{TO}=33.3$ meV, and $\epsilon_\infty=11.1$.[28]

We now examine the reciprocal lifetime with respect to (i) the dispersion of the coupled plasmon–LO-phonon modes and (ii) the electron scattering strength associated with these modes. These properties are modifications of the uncoupled plasmon and LO-phonon mode frequencies and scattering strengths, due to interactions, and can be loosely referred to as "screening" effects. The notions of screening become more difficult to quantify in the Landau damping region.

A. Coupled modes

The longitudinal collective modes of the coupled system are defined by the peaks in $\mathrm{Im}[1/\epsilon_T(\vec{q}, \omega)]$, where ω is real. When the damping is small, it is sufficient to use the roots of $\mathrm{Re}(\epsilon_T)=0$ to estimate the mode frequencies; this approximation can fail in regions where the damping is important.

Figures 2–4 illustrate three different examples of the mode structures. For the wave-vector region of interest the uncoupled LO-phonon mode is assumed to be dispersionless. The uncoupled plasmon dispersion $\omega_p(q)$ in the undamped region is given by the zeros of $\epsilon_e(\vec{q}, \omega)$ and at $q=0$ yields the familiar screened plasma frequency $\omega_p^0 = (4\pi n e^2/m^*\epsilon_\infty)^{1/2}$. In the particle-hole excitation

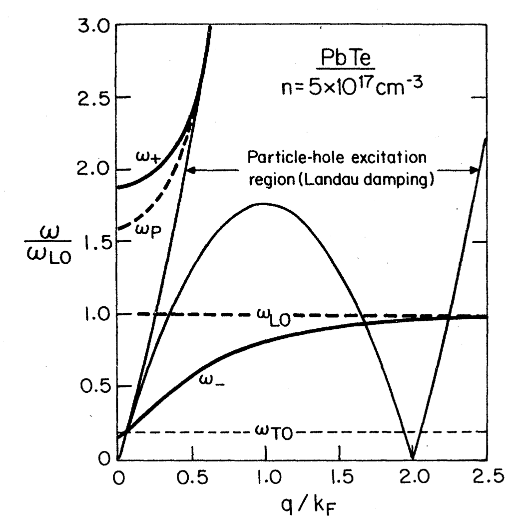

FIG. 2. Dispersion of the longitudinal modes $\omega_\pm$ of the coupled plasmon–LO-phonon system corresponding to the peaks in $\mathrm{Im}[1/\epsilon_T(\vec{q}, \omega)]$. $\omega_{LO}=13.5$ meV, $k_F=1.55\times10^6$ cm^{-1}, $\epsilon_\infty=39$, and $m^*/m_0=0.038$. The dashed lines ω_p and ω_{LO} are the modes of the uncoupled system, the plasmon and the LO phonon, respectively. The line concaved downward is the boundary within which $\mathrm{Im}[\epsilon_e(\vec{q}, \omega)]$ for the Lindhard function is proportional to ω; outside the boundary the imaginary part includes terms in ω^2 and ω.

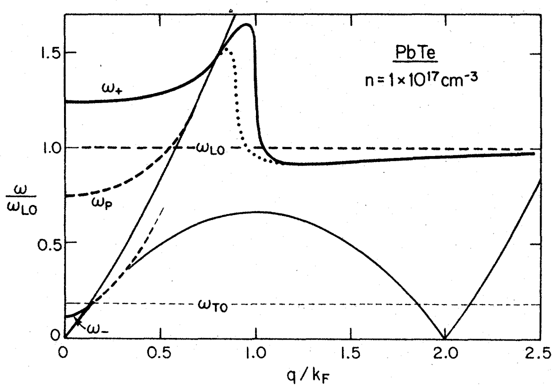

FIG. 3. Dispersion of the coupled plasmon–LO-phonon modes. $k_F = 9.05\times10^5\ \mathrm{cm}^{-1}$ and $m^*/m_0 = 0.035$. The dotted line corresponds to the root of $\mathrm{Re}[\epsilon_T(\vec{q},\omega)]=0$. The fading dashed line for ω_- in the damping region indicates that the corresponding peaks in $\mathrm{Im}(1/\epsilon_T)$ are highly broadened and no longer well defined.

region real solutions of $\epsilon_e(\vec{q},\omega)=0$ no longer exist as the collective plasma excitations are strongly damped out. In the undamped region the coupled modes are described by two branches, denoted by $\omega_+(q)$ and $\omega_-(q)$, with $\omega_\pm(0)$ satisfying

$$\omega_\pm^2(0)=\tfrac{1}{2}\{(\omega_p^{02}+\omega_{\mathrm{LO}}^2)\pm[(\omega_p^{02}+\omega_{\mathrm{LO}}^2)^2-4\omega_p^{02}\omega_{\mathrm{TO}}^2]^{1/2}\}.$$

They correspond to zeros in $\mathrm{Re}(\epsilon_T)$ and δ-functions in $\mathrm{Im}(1/\epsilon_T)$, and in the damped region $\omega_\pm$ have broadened peaks in $\mathrm{Im}(1/\epsilon_T)$.[29] Coupled modes defined from the maximum in $\mathrm{Im}(1/\epsilon_T)$ and from $\mathrm{Re}(\epsilon_T)=0$ can be quite different in the damping region as shown by the solid and dotted lines corresponding to ω_+ in Figs. 3 and 4. Coupled modes in GaAs have been previously characterized in the damping region from the roots of $\mathrm{Re}(\epsilon_T)=0$.[30]

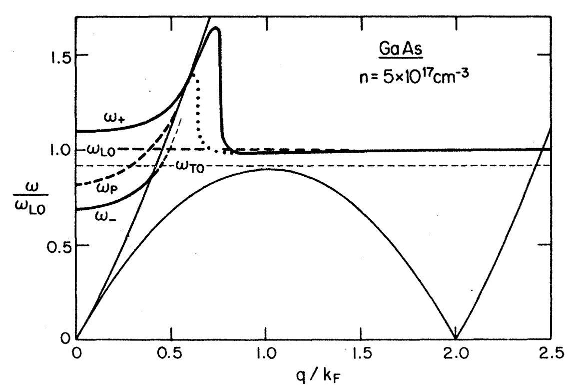

FIG. 4. Dispersion of the coupled plasmon–LO-phonon modes. $\omega_{\mathrm{LO}}=36.3$ meV, $k_F=2.46\times10^6\ \mathrm{cm}^{-1}$, $\epsilon_\infty=11.1$, and $m^*/m_0=0.070$. The dotted line corresponds to the root of $\mathrm{Re}[\epsilon_T(\vec{q},\omega)]=0$. The fading dashed line for ω_- in damping region indicates that the corresponding peaks in $\mathrm{Im}(1/\epsilon_T)$ are highly broadened and no longer well defined.

The coupled modes $\omega_\pm(q)$ are a mixture of collective electron and ion motion. In the undamped region for small q, where $\omega_\pm$ are well defined, the degree of phonon (plasmon) content in these modes can be quantified. We choose to define a phonon strength of the coupled-mode branch ν, denoted by $S_\nu^Q(q)$, such that $\sum_{\nu=\pm}S_\nu^Q=1$. This differs from the phonon strength $S_\nu^{Q'}$ defined by Varga which obeys the sum rule $\sum_{\nu=\pm}(\omega_\nu/\omega_{\mathrm{LO}})S_\nu^{Q'}=1$.[14] Expressions for $S_\nu^Q(q)$ can be obtained as follows. We define $\psi_{\vec{q},\nu}$, the normal coordinate operator for the coupled mode belonging to the νth branch, such that the LO-phonon coordinate operator can be expanded as

$$Q_{\vec{q}}=\sum_{\nu=\pm}a_\nu^Q\,\psi_{\vec{q},\nu}\ . \tag{22}$$

From (22) the renormalized Green's function can be expressed

$$\mathfrak{D}_{QQ}(\vec{q},\omega)=\sum_{\nu=\pm}|a_\nu^Q|^2\mathfrak{D}_{\nu\nu}(\vec{q},\omega)\,, \tag{23}$$

where $\mathfrak{D}_{\nu\nu}$ is the Green's function for the νth coupled-mode branch; the coefficient $|a_\nu^Q|^2$ can be identified as the normalized phonon strength S_ν^Q. Useful expressions for $|a_\nu^Q|^2$ can be obtained by first assuming that $\mathfrak{D}_{\nu\nu}(\vec{q},\omega)$ has the form

$$\mathfrak{D}_{\nu\nu}(\vec{q},\omega)=\hbar/[\omega^2-\omega_\nu^2(q)] \tag{24}$$

and replacing the Lindhard function (20) by its $q\to0$ limit

$$\epsilon_T^{eL}(\vec{q},\omega)\simeq1-\epsilon_\infty\frac{\omega_p^2(q)}{\omega^2}\,, \tag{25}$$

$$\omega_p^2(q)\simeq\omega_p^{02}\left(1+\frac{3}{5}\frac{\hbar^2k_F^2}{m^{*2}\omega_p^{02}}q^2\right),\quad \omega_p^0=\left(\frac{4\pi ne^2}{m^*\epsilon_\infty}\right)^{1/2}.$$

Equating (23) and (8) yields

$$|a_+^Q|^2=(\omega_+^2-\omega_p^2)/(\omega_+^2-\omega_-^2)=S_+^Q(q)\,,$$
$$|a_-^Q|^2=(\omega_p^2-\omega_-^2)/(\omega_+^2-\omega_-^2)=S_-^Q(q)\,, \tag{26}$$

where

$$\omega_\pm^2(q)=\tfrac{1}{2}\big([\omega_p^2(q)+\omega_{\mathrm{LO}}^2]\pm\{[\omega_p^2(q)+\omega_{\mathrm{LO}}^2]^2-4\omega_p^2(q)\omega_{\mathrm{TO}}^2\}^{1/2}\big)\,. \tag{27}$$

[The phonon strength defined by Varga is then given by $(\omega_{\mathrm{LO}}/\omega_\pm)S_\pm^Q$.] A plasmon strength associated with the νth coupled branch can be similarly defined; however, the phonon strength is also indirectly a measure of the plasmon content.

For PbTe $n=5\times10^{17}\ \mathrm{cm}^{-3}$ (Fig. 2), $\omega_p^0/\omega_{\mathrm{LO}}=1.59$. The ω_+ mode is more plasmonlike in character $[S_+^Q(0)\doteq0.28]$ and peaks in $\mathrm{Im}(1/\epsilon_T)$ are no longer distinguishable beyond the Landau damping boundary. The more phononlike ω_- mode enters the particle-hole excitation region at a rather small wave vector and approaches the uncoupled LO-phonon frequency for large wave vectors where the plasma oscillations no longer exist. In the damping region, near the boundary, the dispersion obtained from $\mathrm{Im}(1/\epsilon_T)$ is shifted slightly lower in energy than that obtained from the zeros of $\mathrm{Re}(\epsilon_T)$.

For carrier concentration $n = 1\times10^{17}$ cm^{-3} (Fig. 3), where $\omega_p^0/\omega_{\mathrm{LO}} = 0.74$, the uncoupled modes ω_p and ω_{LO} cross. The coupling splits these modes into ω_+, which is more phononlike $[S_+^0(0) = 0.65]$ and ω_- which is more plasmonlike. Both modes are strongly damped just beyond the boundary where the peaks in $\mathrm{Im}(1/\epsilon_T)$ are essentially washed out. As the plasmon part decays rapidly in this region, the more phononlike ω_+ drops abruptly toward the pure ω_{LO} frequency. For GaAs, $n = 5\times10^{17}$ cm^{-3} (Fig. 4) $[\omega_p^0/\omega_{\mathrm{LO}} = 0.82;\ S_+^0(0) = 0.72]$, the coupled-mode behavior is similar to the lower carrier concentration PbTe with $n = 1\times10^{17}$ cm^{-3} owing to the higher LO-phonon frequency.

B. Coupled-mode scattering strength

In the reciprocal scattering lifetime, Eq. (12), the bare Coulomb potential $4\pi e^2/q^2$ associated with the electrostatic interactions in the system of electrons and LO phonons is modified by $-\mathrm{Im}[1/\epsilon_T(\vec{q},\omega)]$. The combined factors,

$$F_S(\vec{q},\omega) = -(4\pi e^2/q^2)\,\mathrm{Im}[1/\epsilon_T(\vec{q},\omega)]\,, \tag{28}$$

describe the effective scattering strength of the coupled plasmon–LO-phonon modes. We examine the behavior of the scattering strength for the undamped and damped regions.

For small wave vectors, the coupled modes are in the undamped region, and $\mathrm{Im}[1/\epsilon_T(\vec{q},\omega)]$ is described by δ functions occurring at $\omega = \omega_\pm(q)$. We can formulate analytical expressions for the limit $\omega\to 0$ and also for $q\to 0$ in the Lindhard function, Eq. (20).

In the limit of static screening, $\omega_p^0 \gg \omega_{\mathrm{LO}}$, i.e., the vibrations of the ions are quasistatic with respect to the collective electron motion,

$$\begin{aligned} &\epsilon_e(\vec{q},0) = \epsilon_\infty[1 + q_s^2(q)/q^2]\,,\\ &q_s^2(q) = \frac{4\pi e^2}{\epsilon_\infty}\,\frac{m^* k_F}{\hbar^2 2\pi^2}\,2U(q')\,,\quad q' = \frac{q}{k_F}\,,\\ &U(q') = \frac{1}{2}\left[1 + \frac{1}{q'}\left(1 - \frac{q'^2}{4}\right)\ln\left|\frac{1+\frac{1}{2}q'}{1-\frac{1}{2}q'}\right|\right]. \end{aligned} \tag{29}$$

$\epsilon_e(\vec{q},0)$ gives rise to the highly screened LO mode (ω_-) as discussed in Sec. II. $[U(q') = 1$ corresponds to Fermi-Thomas screening or the limit of $\epsilon_e(\vec{q},0)$ as $q\to 0$.]

For the case of dynamic screening where ω_p^0 is comparable to ω_{LO}, the Lindhard function can be approximated, in the limit of small q, by the expressions (25) and (27). Then

$$\epsilon_T(\vec{q},\omega) \simeq \epsilon_\infty\left[1 - \frac{\omega_p^2(q)}{\omega^2} - \left(\frac{\omega_{\mathrm{LO}}^2 - \omega_{\mathrm{TO}}^2}{\omega^2 - \omega_{\mathrm{TO}}^2}\right)\right], \tag{30}$$

which yields

$$\begin{aligned} -\mathrm{Im}(1/\epsilon_T) = \epsilon_\infty^{-1}\,\omega^2(\omega^2 - \omega_{\mathrm{TO}}^2)\\ \times\left[\left(\frac{1}{\omega_+^2 - \omega_-^2}\right)\frac{\pi}{2\omega_+}[\delta(\omega-\omega_+) - \delta(\omega+\omega_+)] + \left(\frac{1}{\omega_-^2 - \omega_+^2}\right)\frac{\pi}{2\omega_-}[\delta(\omega-\omega_-) - \delta(\omega+\omega_-)]\right]. \end{aligned} \tag{31}$$

Substituting (31) into (12) and integrating over $d\hbar\omega$

$$\begin{aligned} \tau^{-1}(\vec{k},n) = \frac{2\pi}{\hbar}\int\frac{d\vec{q}}{(2\pi)^3} f_{\vec{k},n}(1 - f_{\vec{k}-\vec{q},n})(1 + n_{\omega_\pm})\,|F^{nn}_{\vec{k},\vec{k}-\vec{q}}|^2\\ \times\frac{4\pi e^2}{q^2}\left[\frac{\hbar\omega_+}{2\epsilon_\infty}\left(\frac{\omega_+^2 - \omega_{\mathrm{TO}}^2}{\omega_+^2 - \omega_-^2}\right)\delta(\hbar\omega_+ + E_{\vec{k}-\vec{q},n} - E_{\vec{k},n}) + \frac{\hbar\omega_-}{2\epsilon_\infty}\left(\frac{\omega_-^2 - \omega_{\mathrm{TO}}^2}{\omega_-^2 - \omega_+^2}\right)\delta(\hbar\omega_- + E_{\vec{k}-\vec{q},n} - E_{\vec{k},n})\right]. \end{aligned} \tag{32}$$

Comparing the scattering strength corresponding to (31) with that of the unscreened Fröhlich scattering function obtained from (13), characteristics of dynamic screening can be seen for small q. The ratio of the screened $F_s^s(\omega_\pm)$ to unscreened Fröhlich scattering strength F_s^u, $F_s^s(\omega_\pm)/F_s^u$, can be obtained from Eqs. (32) and (14) as

$$\frac{F_s^s(\omega_\pm)}{F_s^u} = \left(\frac{\epsilon_0}{\epsilon_0 - \epsilon_\infty}\right)\frac{\omega_\pm}{\omega_{\mathrm{LO}}}\left(\frac{\omega_\pm^2 - \omega_{\mathrm{TO}}^2}{\omega_\pm^2 - \omega_\mp^2}\right). \tag{33}$$

Since ω_+ and ω_- are essentially dispersionless for $q/k_F \lesssim 0.1$, we examine the behavior of $F_s^s(\omega_\pm)/$

TABLE I. Ratio of the screened scattering strength $F_s^s(\omega_\pm)$ to the unscreened Fröhlich scattering strength F_s^u, where $F_s^s(\omega_\pm)/F_s^u$ is given by Eq. (33). S_+^Q is the phonon strength of the mode ω_- ($S_-^Q = 1-S_+^Q$). The computed values are for $q = 0$.

Semiconductor	n (10^{18}cm^{-3})	$\frac{\omega_p^0}{\omega_{LO}}$	$\frac{\omega_+}{\omega_{LO}}$	S_+^Q	$\frac{\omega_-}{\omega_{LO}}$	$\frac{F_s^s(\omega_+)}{F_s^u}$	$\frac{F_s^s(\omega_-)}{F_s^u}$
PbTe	0.1	0.74	1.24	0.65	0.111	1.27	1.65×10^{-3}
$\left(\frac{\omega_{TO}}{\omega_{LO}}=0.185\right)$	0.5	1.59	1.87	0.28	0.157	1.93	4.47×10^{-4}
	1.0	2.18	2.39	0.17	0.169	2.47	1.77×10^{-4}
	5.0	4.31	4.42	0.05	0.180	4.58	1.65×10^{-5}
GaAs	0.5	0.82	1.10	0.72	0.686	3.41	2.20
$\left(\frac{\omega_{TO}}{\omega_{LO}}=0.917\right)$							

F_s^u in this region using values computed at $q=0$. The results are listed in Table I for selected carrier concentrations. For PbTe, the ω_+ modes, which are mainly plasmon in character ($S_+^Q \le 0.28$), have large $F_s^s(\omega_+)/F_s^u$ due to their high frequencies compared to ω_{LO}, and to the fact that these modes are screened primarily by ϵ_∞. The corresponding ω_- modes, which are mainly phonon, have $F_s^s(\omega_-)/F_s^u \ll 1$ reflecting the effects of screening by the free-carrier system. For ω_+ modes in PbTe and GaAs, which are more phononlike ($S_+^Q = 0.65$ and 0.72), the scattering strength ratio is also greater than unity. The "antiscreening" effect is essentially due to the fact that $\omega_+/\omega_{LO} > 1$. The corresponding ω_- modes are then mainly plasma motion screened by the static dielectric constant ϵ_0. For PbTe $\epsilon_0 \sim 10^3$, which accounts for $F_s^s(\omega_-)/F_s^u \ll 1$. However, for GaAs $\epsilon_0 \sim 13$. In addition, ω_{LO} and ω_{TO} (hence ϵ_0 and ϵ_∞) are rather similar. These lead in Eq. (33) to a scattering ratio greater than unity, although still less than that of ω_+.

In many transport processes electron scattering is governed by larger wave-vector transfers that occur in the Landau damping region. We next study the behavior of the scattering strength $F_s(\vec{q}, \omega)$ for the more phononlike mode in PbTe as affected by Landau damping. The peaks in $\mathrm{Im}(1/\epsilon_T)$ are still well defined in the damping region for this mode, whereas it is washed out for the more plasmonlike mode. The scattering strength tends to be highly dispersive with respect to energy and wave-vector transfers in the damping region. Damping broadens the scattering strength about the resonant coupled-mode frequencies, while screening tends to modify the amplitude of the scattering strength corresponding to the mode frequency. For finite temperatures the low-energy tail of the broadened $F_s(\vec{q}, \omega)$ may contribute appreciably to the scattering due to the boson population factor. Figure 5 illustrates these effects for $n = 5\times10^{17}$ cm^{-3}, where ω_- is more phononlike. Figures 6 and 7 correspond to ω_+ more phononlike, $n = 1\times10^{17}$ cm^{-3}. In Fig. 5, the broad-

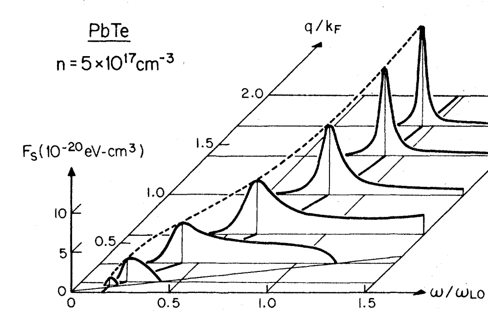

FIG. 5. Dispersion of the coupled-mode scattering strength

$$F_s(\vec{q}, \omega) = -(4\pi e^2/q^2)\,\mathrm{Im}[1/\epsilon_T(\vec{q}, \omega)]$$

for ω_- more phononlike. The peaks correspond to ω_- in Fig. 2.

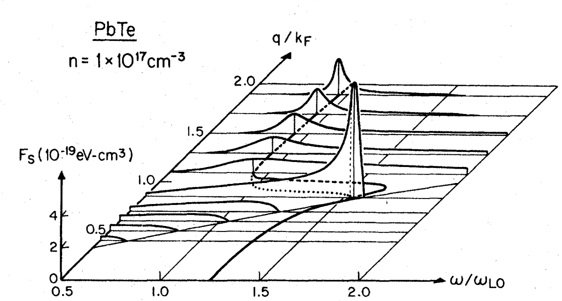

FIG. 6. Dispersion of the coupled-mode scattering strength $F_s(\vec{q}, \omega)$ for ω_+ more phononlike. The dotted line corresponds to the solution of $\mathrm{Re}[\epsilon_T(\vec{q}, \omega)] = 0$. The peaks correspond to ω_+ in Fig. 3.

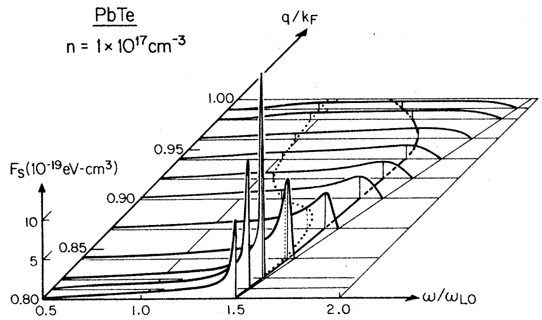

FIG. 7. Expanded view of Fig. 6 for the region $0.8 \leqslant q/k_F \leqslant 1.0$.

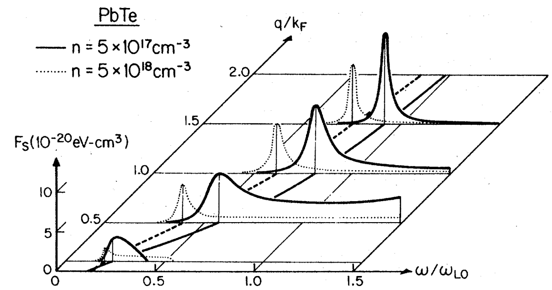

FIG. 8. Dispersion of the coupled-mode scattering strength $F_s(\vec{q}, \omega)$ for ω_- more phononlike, for two carrier densities. The normalized wave vector is in units of k_F for $n = 5 \times 10^{17}$ cm^{-3}.

ening of ω_- is asymmetrical, extending toward the more plasmonlike ω_+. In Fig. 6, the highly broadened F_s for $q/k_F \lesssim 0.8$ corresponds to the more plasmonlike ω_-.

The mode broadening due to damping by the particle-hole excitations is particularly strong near the damping boundary for either ω_+ or ω_- more phononlike. This is most pronounced for the wave-vector region $q/k_F \sim 1$ (see Figs. 6 and 7), where the ω_+ mode abruptly approaches the uncoupled ω_{LO} frequency. For large wave vectors $q \sim 2k_F$, where the plasmon excitations have all but vanished, the width of the modes sharpens toward a δ function associated with the pure, undamped ω_{LO}.

In the damping region, screening effects cannot be simply isolated as in the case of the coupled modes in the undamped region. However, features characteristic of screening can be seen in the behavior of the scattering function F_s. For larger wave vectors, F_s associated with either ω_+ or ω_- more phononlike increases as ω_{LO} is approached. Also as the carrier concentration is increased by an order of magnitude from 5×10^{17} cm^{-3}, a reduction in F_s, as well as a frequency shift in ω_-, reflect screening effects, as shown by Fig. 8.

IV. SUMMARY AND CONCLUSIONS

We have presented a generalized formulation of the electron-scattering interaction with coupled plasmon–LO-phonon modes in degenerate polar semiconductors. The scattering lifetime was derived for this interaction in terms of a dielectric response formalism and was shown to treat effects of strong mode coupling and Landau damping. Coupled modes and the associated scattering strength were evaluated for PbTe and GaAs and found to be highly dispersive with respect to energy and wave-vector transfers.

The role of Landau-damped coupled modes appears to be particularly important in characterizing electron transport in degenerate semiconductors where $\omega_p^0 \sim \omega_{LO}$. The corresponding highly dispersive coupled-mode scattering strength makes available a larger portion of the energy-wave-vector space to contribute to scattering, compared to the undamped case. At finite temperatures, the mode broadening could make the low-energy tail of the scattering strength contribute appreciably to scattering, via the boson population factor. It seems essential to take into account the damped coupled mode behavior in characterizing low-field electron transport as well as high-field effects, such as hot electrons and saturation velocities. Such treatments would be in order.

In a separate work we will illustrate the useful application of the generalized scattering formulation presented here to help explain low-field transport effects in the narrow-gap semiconductors $Pb_{1-x}Sn_xTe$.

ACKNOWLEDGMENTS

The authors would like to thank Professor A. C. Smith and Professor D. Adler for informative discussions and helpful comments regarding the manuscript. This work was supported by the NSF under Grant No. DMR-76-80895. One of the authors (M.E.K.) would like to thank the IBM Corporation for postdoctoral support.

*Present address: Science Center, Rockwell International, Thousand Oaks, Calif. 91360.

[1]H. Fröhlich, Proc. R. Soc. A 160, 230 (1937).
[2]F. E. Low and D. Pines, Phys. Rev. 98, 414 (1955).
[3]H. Ehrenreich, J. Phys. Chem. Solids 2, 131 (1957).
[4]H. Ehrenreich, J. Phys. Chem. Solids 8, 130 (1959).
[5]Yu. I. Ravich, B. A. Efimova, and V. I. Tarmarchenko, Phys. Status Solidi B 43, 11 (1971).
[6]T. P. McLean and E. G. S. Paige, J. Phys. Chem. Solids 16, 220 (1960).
[7]J. Appel, Phys. Rev. 122, 1760 (1961).
[8]M. E. Kim, A. Das, and S. D. Senturia, Bull. Am. Phys. Soc. 22, 599 (1977).
[9]P. Wolff, Phys. Rev. 126, 405 (1962).
[10]J. Lindhard, K. Dan. Vidensk. Selsk. Mat. Fys. Medd. 28, 8 (1954).
[11]H. Ehrenreich and M. H. Cohen, Phys. Rev. 115, 786 (1959).
[12]J. J. Quinn, Phys. Rev. 126, 1453 (1962).
[13]P. Nozières and D. Pines, Nuovo Cimento 9, 470 (1958).
[14]B. B. Varga, Phys. Rev. 137, A1896 (1965).
[15]K. S. Singwi and M. P. Tosi, Phys. Rev. 147, 658 (1966).
[16]R. Rabitz and B. Lax, J. Phys. Chem. Solids 32, 359 (1971).
[17]L. Van Hove, Phys. Rev. 95, 249 (1954).
[18]See, for example, A. L. Fetter and J. D. Walecka, *Quantum Theory of Many-Particle Systems* (McGraw-Hill, New York, 1971), p. 227.
[19]L. D. Landau, J. Phys. (U.S.S.R.) 10, 25 (1946).
[20]D. K. Ferry, Phys. Rev. B 9, 4277 (1974).
[21]R. A. Cowley and G. Dolling, Phys. Rev. Lett. 14, 549 (1965).
[22]D. F. DuBois, Ann. Phys. 8, 24 (1959).
[23]M. S. Adler, C. R. Hewes, and S. D. Senturia, Phys. Rev. B 7, 5186 (1973).
[24]H. A. Alperin, S. J. Pickart, J. J. Rhyne, and V. J. Minkiewicz, Phys. Lett. 40A, 295 (1972).
[25]S. G. Bishop and B. W. Henvis, Solid State Commun. 7, 437 (1969).
[26]S. Perkowitz, Phys. Rev. B 12, 3210 (1975).
[27]J. R. Lowney and S. D. Senturia, J. Appl. Phys. 47, 1771 (1976).
[28]A. Mooradian and G. B. Wright, Solid State Commun. 4, 431 (1966).
[29]L. F. Lemmens, F. Brasens, and J. T. Devreese, Solid State Commun. 17, 337 (1975).
[30]L. F. Lemmens and J. T. Devreese, Solid State Commun. 14, 1339 (1974).